

# The WIYN One Degree Imager 2014: Performance of the Partially Populated Focal Plane and Instrument Upgrade Path

Daniel R. Harbeck<sup>a</sup>, Todd Boroson<sup>b,c</sup>, Michael Lesser<sup>d</sup>, Jayadev Rajagopal<sup>b</sup>, Andrey Yeatts<sup>a</sup>, Charles Corson<sup>b</sup>, Wilson Liu<sup>a</sup>, Ian Dell'Antonio<sup>e</sup>, Ralf Kotulla<sup>f,g</sup>, David Ouellete<sup>d</sup>, Eric Hooper<sup>a,g</sup>, Mike Smith<sup>g</sup>, Richard Bredthauer<sup>h</sup>, Pierre Martin<sup>i</sup>, Gary Muller<sup>j</sup>, Patricia Knezek<sup>k</sup>, Mark Hunten<sup>l</sup>

<sup>a</sup> WIYN Observatory, Tucson, AZ (USA), <sup>b</sup> National Optical Astronomy Observatory, Tucson, AZ (USA), <sup>c</sup> Las Cumbres Observatory Global Telescope Network, Goleta, CA (USA), <sup>d</sup> The University of Arizona, Tucson, AZ (USA), <sup>e</sup> Brown University, Providence, RI (USA), <sup>f</sup> University of Wisconsin, Milwaukee, WI (USA), <sup>g</sup> University of Wisconsin, Madison, WI (USA), <sup>h</sup> Semiconductor Technology Associates, Inc., San Juan Capistrano, CA (USA), <sup>i</sup> University of Hawaii, Hilo, HI (USA), <sup>j</sup> GMTO Corporation, Pasadena, CA (USA), <sup>k</sup> National Science Foundation, Arlington, VA (USA), <sup>l</sup> Lunar and Planetary Laboratory, Tucson, AZ (USA)

## ABSTRACT

The One Degree Imager (ODI) was deployed during the summer of 2012 at the WIYN 3.5m telescope, located on Kitt Peak near Tucson, AZ (USA). ODI is an optical imager designed to deliver atmosphere-limited image quality ( $\leq 0.4''$  FWHM) over a one degree field of view, and uses Orthogonal Transfer Array (OTA) detectors to also allow for on-chip tip/tilt image motion compensation. At this time, the focal plane is partially populated ("pODI") with 13 out of 64 OTA detectors, providing a central scientifically usable field of view of about  $24' \times 24'$ ; four of the thirteen detectors are installed at outlying positions to probe image quality at all field angles. The image quality has been verified to be indeed better than  $0.4''$  FWHM over the full field when atmospheric conditions allow. Based on over one year of operations, we summarize pODI's performance and lessons learned. As pODI has proven the viability of the ODI instrument, the WIYN consortium is engaging in an upgrade project to add 12 more detectors to the focal plane enlarging the scientifically usable field of view to about  $40' \times 40'$ . A design change in the new detectors has successfully addressed a low light level charge transfer inefficiency.

**Keywords:** Ground based instrumentation, wide field imaging, CCD, Orthogonal Transfer Array

## 1. INTRODUCTION

The One Degree Imager (ODI) is an optical imager for the WIYN 3.5m telescope located at Kitt Peak near Tucson, AZ (USA), utilizing Orthogonal Transfer Array CCD detectors. The intrinsic field of view of the instrument is one degree square, where the central one degree circle is unvignetted. ODI's optical and mechanical design as well as status have been documented in detail in previous SPIE publications.<sup>1-9</sup> Here we report on the status and operational performance of ODI, which was deployed at the WIYN telescope in summer 2012 with a partially populated focal plane (called "pODI"). Thus, ODI as an instrument is complete, but for the full complement of detectors in the focal plane.

In this paper we will first give a brief overview of the instrument and describe the performance of the detectors and focal plane, and illustrate the performance of the entire instrument and the data flow at the telescope. Finally we will describe an ongoing project to upgrade the focal plane to a  $5 \times 5$  detector array, which will provide an  $\sim 40' \times 40'$  field of view.

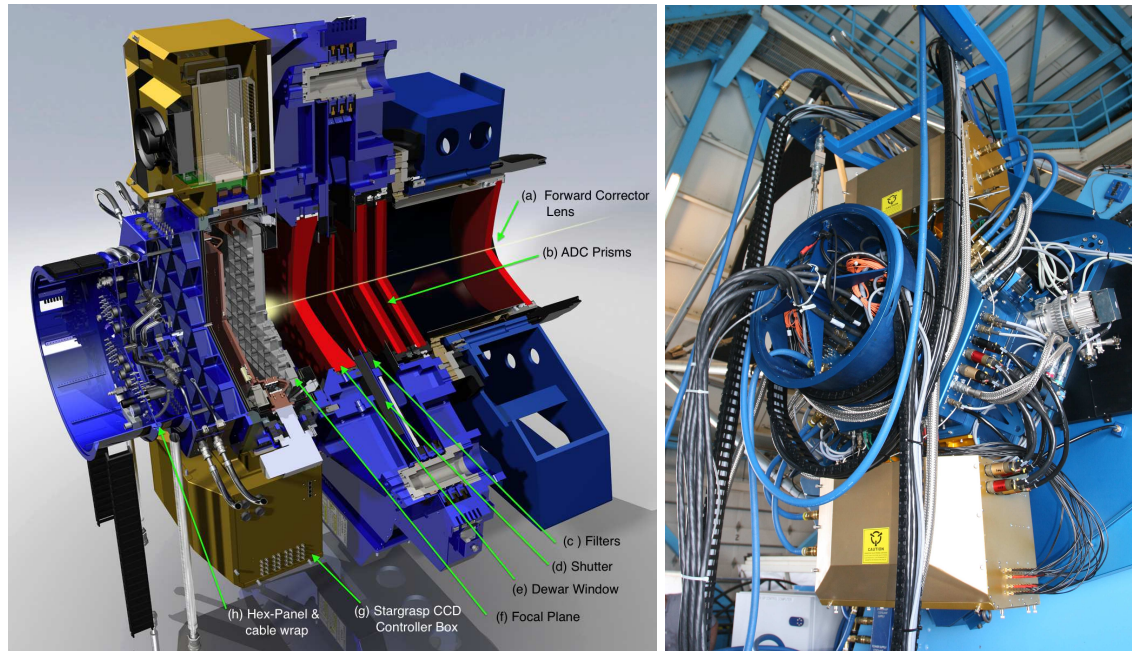


Figure 1. Left: Section view through ODI Model. Light enters from the telescope (right) through the forward corrector lens (a), then passes the two prisms of the atmospheric dispersion compensator (b) and one of the nine filters (c). Following the filters the shutter (d) is mounted just in front of the dewar window (e); note that the dewar window also has optical power. In the dewar the detectors are mounted on the focal plane (f). Noticeably mounted on the sides of the dewar are the two golden Stargrasp CCD controller boxes (g). The hex panel and cable wrap (h) are mounted on the back of the instrument. Right: ODI mounted at the WIYN 3.5m telescope.

## 2. INSTRUMENT OVERVIEW

ODI consists of the instrument body that is mounted to the Nasmyth port of the WIYN telescope plus supporting infrastructure throughout the WIYN facility. Key elements of the instrument body are (shown in Fig. 1): Two rotatable prisms form an **atmospheric dispersion compensator**. Each prism is driven by a stepper motor. **Nine filter arms** can move into the telescope beam like a semaphore. The filter arms are mounted to three supporting posts; on each post there are three filter arms mounted in three layers. The shutter was created by the University of Bonn.

The **dewar** is mounted to the instrument support package. Its main component is the vacuum vessel with the focal plane. The dewar window is also an optically powered element, and forms the field flattener in conjunction with the forward corrector lens. The focal plane, with up to 64 OTA detectors, is cooled by four closed-cycle helium cryo-heads that are capable of removing 200W of heat from the focal plane (130 W for a full set of 64 OTA detectors, plus about 60W radiative load). A turbo-molecular vacuum pump is permanently mounted to the dewar.

The **CCD controllers** (IfA Stargrasp controllers<sup>10</sup>) are mounted on two opposite sides of the dewar, and each side drives one half of the detector array on the focal plane. Since the CCD controllers dissipate a significant amount of heat (1.2kW), they are enclosed in isolated, glycol-cooled boxes to avoid creating a turbulent air flow in the dome (and thus degrading the seeing). The back of the dewar carries a cable wrap for control lines and power supplies.

## 3. FOCAL PLANE PERFORMANCE

ODI uses Orthogonal Transfer Array (OTA) detectors<sup>11</sup> that have been custom-designed by Semiconductor Technology Associates (STA), and processed and packaged<sup>9</sup> by Imaging Technology Lab of the University of Arizona. Each detector die is divided into an  $8 \times 8$  array of semi-independent detector cells with  $480 \times 496$  pixels each.

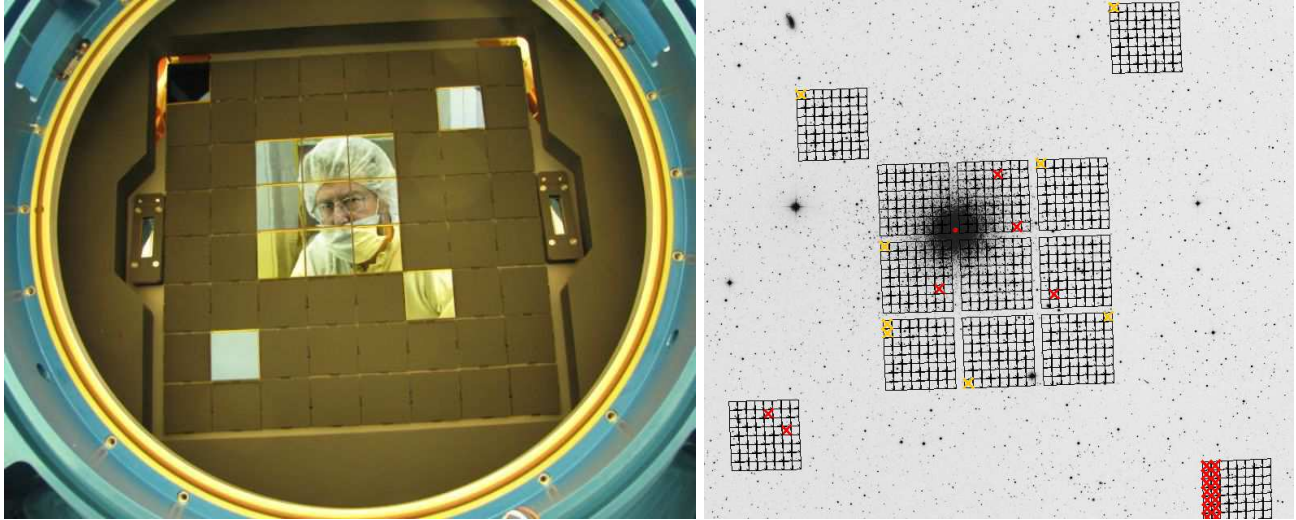


Figure 2. In pODI, 13 detectors are mounted on the focal plane (left). The imprint on the sky is shown right; in this image north is up, east is left. In the imprint map, defective OTA cells are marked with red crosses.

With a pixel size of  $12\mu\text{m}$  and a pixel scale of  $0.1''$  per pixel, each cell covers a little under  $1' \times 1'$  on sky, or  $8' \times 8'$  per detector die. The gaps size between individual cells is  $3''$  and  $2''$  in the x- and y- directions, respectively.

Each cell of a detector die can be individually controlled, i.e., it is possible to continuously readout some cells in video mode (e.g., for guiding), whereas the remaining cells can be used to integrate the science exposure with a final readout. While integrating, cells can also be commanded to shift charge in all four directions. This feature can be used to provide fast on-chip image tip/tilt motion compensation when used in combination with the video mode readout to probe the image motion of a bright star. A design driver for OTA detectors was the ability to sense image motion on bright stars while applying a tip/tilt motion correction to nearby cells within an isokinetic patch, i.e., to provide a rubber focal plane<sup>12</sup> that follows the image distortions on the sky, and hence improve the delivered image quality.

There are currently thirteen out of a possible sixty-four detectors mounted in pODI. As pODI was intended to be both a demonstration of the instrument's capability, as well as providing a new scientific capability to the observatory, the thirteen detectors have been arranged in a central  $3 \times 3$  array to provide a continuous science field of view of  $24' \times 24'$ , and four outlying detectors probe all field angles in order to verify the performance of the corrector optics (see Figure 2). Vacant locations in the focal plane have been covered with black-painted shields to avoid stray light reflections of the focal plate.

The read noise of the focal plane is detector limited; as each cell in each detector has its own output amplifier, there is no single value for the read noise and gain. In fact, due to varying circuit length on the detector die, the amplifier gain varies significantly with location on the detectors. The gain and read noise of each cell of each detector in the ODI focal plane are shown in a heat map representation in Figure 3. The range in read noise per cell is from  $6e^-$  to  $10e^-$  with a mode at about  $8e^-$ . The dark current of the detectors peaks at  $0.006e^-/\text{pix}/\text{sec}$  with a variance of  $0.002 (e^-/\text{pix}/\text{sec})^2$ .

Binning of pixels allows an observer to virtually increase the pixel size, and hence minimize the time needed to reach sky-noise limited exposures. At this time, pixel binning is only deployed in the parallel readout direction, while binning in the serial readout direction would increase the effective readnoise by more than a factor of  $\sqrt{2}$ , hence invalidating the noise benefits of binning. The underlying issue is not fully understood yet; there is an indication that  $\frac{1}{7}$  noise of the A/D converters in the CCD controllers, at least under the current operating scheme, could contribute to the elevated noise levels when binning. We are working with the Stargrasp controller group to devise a modified operating schema for the A/D converter.

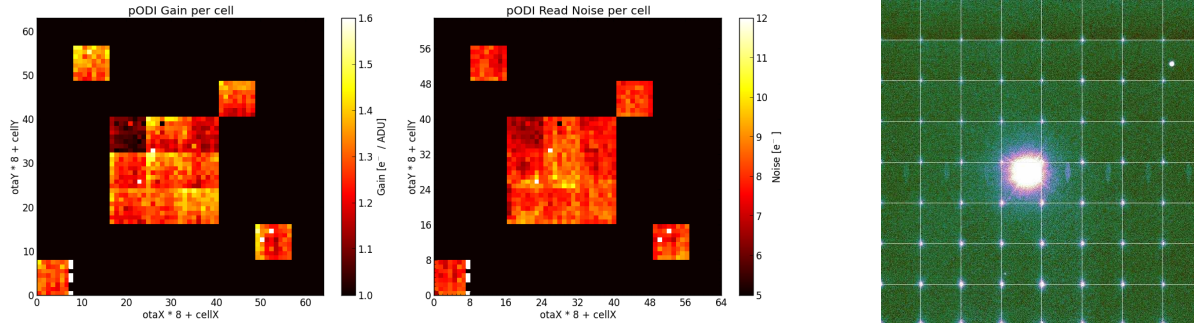


Figure 3. Representation of gain (left) and read noise (right) of each cell of the thirteen detectors in ODI's focal plane. Cross talk in pODI, as demonstrated by a saturated image of a star on the right, is constrained to adjacent cell within an OTA detector.

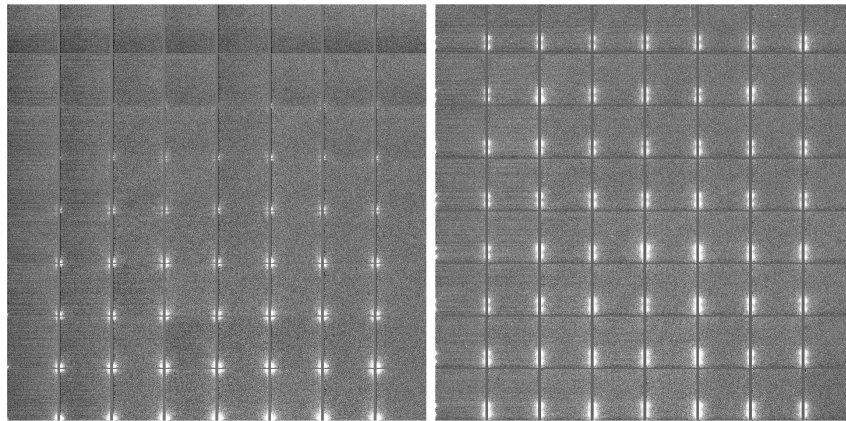


Figure 4. Example of transistor glow in a new implant level Lot 6 OTA device. Output amplifier glow in a bias with control of output drain (left), and pass-transistor glow in a 900 second dark exposure (right). Both images scaled identically.

**Transistor Glow & Detector Operation** Transistor glow in ODI's OTA detectors remains the major limitation. The most significant source of glow is the transistors in the output amplifiers of each cell. Their glow is prohibitively high, and would dominate every exposure with exposures times longer than one minute. A work-around applied in pODI to control the amplifier glow is to reduce the drain voltage of the output amplifiers from typically 24V to 10V during integration and idle times, and power the amplifiers on only while detectors are read out. Therefore, output amplifier glow is limited to the time required to read out the detector, and can be calibrated out of the image like a bias effect; an example bias is shown in Figure 4, left.

Each readout operation, including guide star video readout, requires the output drain for an entire detector to power up, and hence each detector that is used to acquire guide star signals will not be usable for science integration due to the amplifier glow. In order to enable guide operation, at least one entire detector must be sacrificed for guiding an exposure. Using local, atmosphere-induced image motion detection and compensation is therefore impossible for pODI's OTA detectors, as acquiring a guide signal would require a powered-up output drain, and the amplifier glow would outshine the objects on that very detector.

In order to switch between science integration and active video / OT shifting mode, the parallel clocks for each cell can be driven by either a standby parallel voltage, or actively clocked parallel signals. The multiplexing between these two parallel voltages is handled by pass-transistors, and these also glow, albeit at a lower level than the transistors in the output amplifiers. This glow is present in each exposure, independent of the state of output drain. In a long exposure ( $\geq 10$  minutes exposure time), pass transistor glow is comparable to the residual amplifier glow, see Figure 4. The pass transistor glow signature is effectively removed using dark calibration images that are scaled by exposure time.

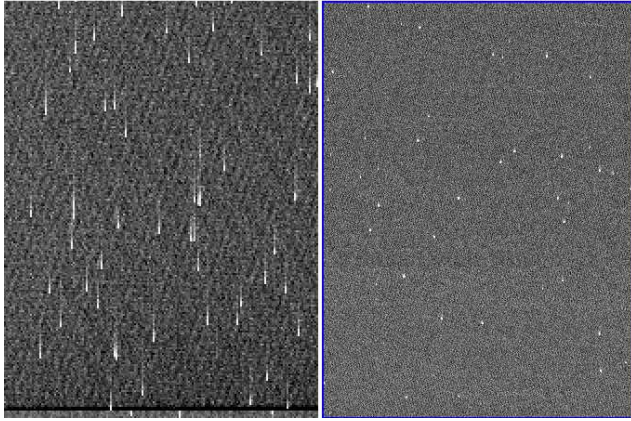


Figure 5. Illustration of charge transfer efficiency using Iron-55 X-ray illuminated images. Under low background conditions, pODI's Lot 6 detectors (left) show significant vertical smearing of single-pixel X-ray events. The revised Lot 7 detectors correct this problem (right).

#### 4. LOW LIGHT LEVEL CHARGE TRANSFER EFFICIENCY

A reduced charge transfer efficiency (CTE) under low light levels has been identified in the Lot 6 detectors, resulting in vertically distributed charge when the background level is lower than  $100e^-$ . The effect is illustrated in Figure 5, which shows an Iron-55 X-ray exposure of current Lot 6 and revised Lot 7 detectors. Since the severity of the CTE is independent of the location within a OTA cell, the underlying cause was readily identified as a charge trap between the first pixel row and the serial register. In a new detector revision (Lot 7) this issue has been addressed by a minor design change in which the buried channels near the serial to parallel transfer have been widened. As demonstrated in Fig 5, the CTE problem has been fully corrected in the latest OTA design revision. The detector dies of Lot 7 are under processing into functional detectors for future upgrade of the ODI instrument (see Section 7).

The low light level CTE of the current Lot 6 detectors has significant impact on the observing strategy with pODI, limiting its viability in some areas:

1. **The minimum exposure time** to reach the minimum background level of  $\approx 100e^-$  is, at a median read noise of  $8e^-$ , comparable to the time to obtain sky-noise limited exposures. Nevertheless, for short exposures with low background, as is the case observations of bright objects, calibrating images with fainter secondary standards in the field is problematic. Furthermore, narrow band or UV imaging with the Lot 6 detectors requires long exposure times ( $\geq 10 - 15$  min) to reach a sufficient background level in a single exposure. This requirement conflicts with the need to extensively dither with pODI if homogeneous field coverage is desired.
2. **Bias and dark** calibration images do have limited background levels, and isolated features, such as amplifier glow or the first few rows of an image, will be affected by the CTE. Programs aiming to observe very low surface brightness features will be limited.
3. **Astrometry** of faint targets shows a systematic trend with the magnitude of objects. In particular when the background level is low, it can shift an object's centroid by about 0.5 pixels in the parallel readout direction, whereas there is no trend noticeable in the serial readout direction. Under sufficiently high background levels this issue is less pronounced, but high accuracy astrometry (e.g., for proper motion measurements), require careful calibration of the CTE impact on centroids.

As the low light level CTE has been resolved for the latest Lot 7 design iteration, the limitations on scientific observations listed above will not apply to this next generation of detectors.

### 5. INSTRUMENT PERFORMANCE

#### 5.1 Image Quality

A major motivation to build ODI was to exploit WIYN's excellent image quality, which can be  $\leq 0.4''$  in optical wavelengths under the best circumstances, over the full one degree field of view. The outlying detectors were

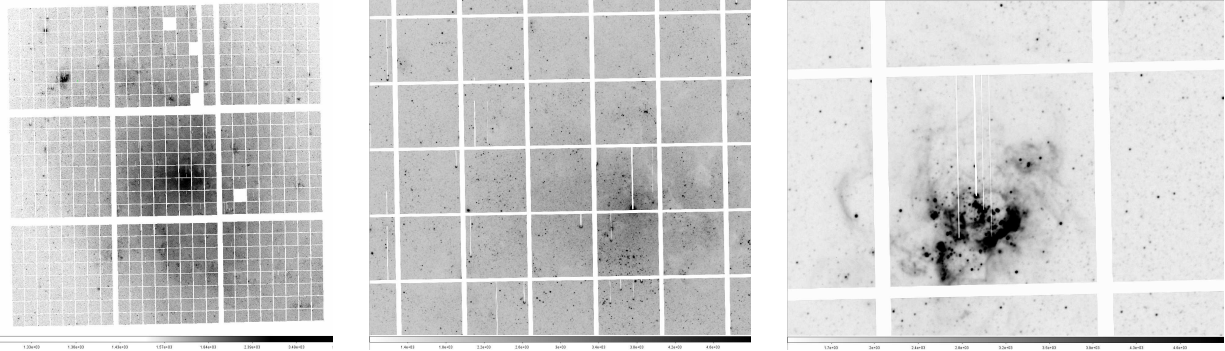


Figure 6. The best image quality delivered by pODI is  $\leq 0.4''$ , as exemplified by an 180 second SDSS  $r'$  band exposure of the Local Group spiral galaxy M33. The left side shows the central  $3 \times 3$  detector science array with a total field of view of about  $24' \times 24'$ ; the image stretch is logarithmic. The middle and right images zoom into the center region of M33 and a star formation region, respectively; their stretch is linear. The calibration pipeline has masked out blooming trails of saturated objects.

placed to verify the instrument performance over all field angles. Contributing factors to the delivered image quality are (i) optics quality, which has been independently verified, (ii) optics alignment, which was verified independently using computer-generated holograms, (iii) focal plane flatness, which was verified to be  $\leq 20\mu\text{m}$ ,<sup>9</sup> and (iv) instrument flexing under varying gravity vectors.

The best delivered image quality for long exposures so far has been  $\leq 0.4''$  FWHM in the SDSS  $r'$  band with no systematic variations over the field of view that would indicate misalignment of the instrument. Example images illustrating ODI's superb image quality are shown in Fig.6. The best PSF based on the shift and add average of four 50ms exposures was measured at  $0.26''$  FWHM, verifying that ODI's image quality is only limited by the atmospheric conditions.

As a means of quantitative characterization of the optical quality of the WIYN telescope and ODI system, on-axis wave front errors have been measured in the SDSS  $r$ -band using in and out of focus images near the optical axis. The defocused images have been processed using wavefront curvature analysis, and the overall wavefront errors were modest, with the strongest contributors being Coma ( $Z7 = 91$  nm rms) and Trefoil ( $Z10 = 140$  nm rms). These wavefront errors are comparable to those seen with other instruments at the WIYN telescope.

The uniformity and stability of the PSF of pODI makes it well-suited for weak lensing studies. The delivered image quality varies by  $\lesssim 5\%$  across the pODI field. The camera delivers images with ellipticities 1-5% across the field, and focus is maintained across sequences of exposures, allowing simultaneous fitting of the PSF pattern using the stars at all dithered positions. Resulting galaxy ellipticities are reproducible to better than 1%. Measurements of Abell 992<sup>13,14</sup> demonstrate the ability to reconstruct mass distributions even for lower redshift clusters.

## 5.2 Throughput and long-term trends

Under ideal conditions, when the telescope mirrors and dewar window are cleaned, the throughput of ODI is close to the prediction. The photometric zero points in the SDSS  $g'$ ,  $r'$ ,  $i'$ , and  $z'$  filters are 26.6, 26.6, 26.1, and 25.2 magnitudes in units of electrons per second and normalized to an airmass of one, respectively. All zeropoints are given in the AB magnitude system.

The photometric zeropoint for the SDSS  $u'$  band has not been measured thoroughly. A proxy zeropoint measurement has been made using a Johnson U band filter (KPNO U solid); this filter has a similar bandpass in combination with the ODI optics as a SDSS  $u$ -band, but is skewed towards longer wavelengths. A proxy AB system zeropoint, when calibrated against SDSS  $u'$  band photometry, is estimated to  $26.3 \pm 0.5$ . Below we describe a strong time variation of the telescope / ODI system throughput; we have seen significant throughput degradation in the UV due to issues with telescope and instrument optics.

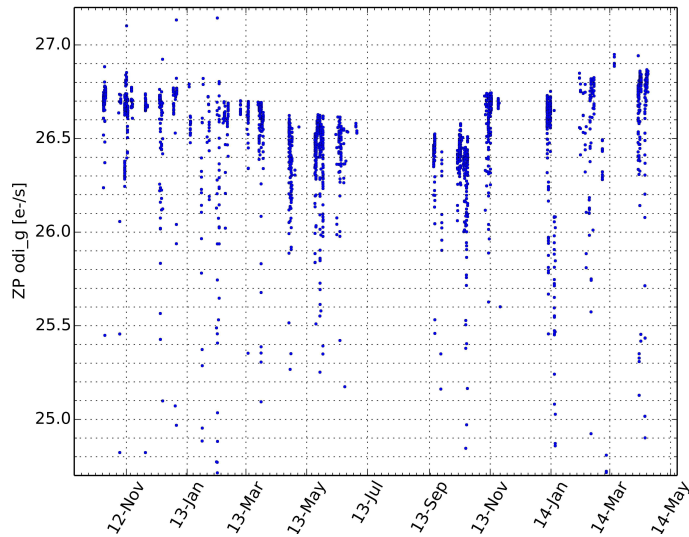


Figure 7. Airmass-corrected photometric zeropoint as measured in the odi g' band for all ODI exposures that were calibrated to the SDSS star catalog. Outstanding events are (i) realuminisation of the secondary mirror in October 2013, and (ii) washing of the primary and tertiary mirror surfaces January 2014.

ODI is a novelty at WIYN in the sense that all data are centrally stored and calibrated, which, for the first time, enables us to monitor the telescope performance based on a very large data set. With a time baseline of over one and a half years of operations, we have identified interesting trends in the photoelectric zeropoints of ODI. Figure 7 shows the trend of the photometric zeropoint in all ODI g' band images that were calibrated against the SDSS DR8 catalog;<sup>15</sup> all zeropoints have been corrected to an airmass of one. While the scatter in the zeropoint distribution is large (attributed to a mixture of non-photometric conditions, deliberate non-sidereal tracking, and calibration errors), the upper envelope of the trend is significant and is mirrored in all four ODI broad band filters (SDSS g', r', i', and z'), with a decreasing amplitude of the overall trend with increasing wavelength.)

A degradation in throughput is evident between November 2012 and October 2013. The throughput improvement of 0.3 mag in October 2013 marks the realuminisation of WIYN's secondary mirror. The second, smaller throughput improvement in January 2014 correlates with more rigorous washing of WIYN's primary and tertiary mirrors in combination with cleaning of the ODI dewar window, which had accumulated residuals from condensation events. Since January 2014, a weekly CO<sub>2</sub> snow cleaning protocol of the telescope mirrors has been followed, and the throughput trend remains flat or improving thereafter. The CO<sub>2</sub> cleaning helps to prevent new particulate accumulation and mitigates the risk of severe contamination events for which soap and water washing is then required to regain throughput. Throughput monitoring with ODI is underlining the importance of regular mirror maintenance at Kitt Peak, where elevated levels of particulates, episodes of high humidity, and the open structure of the WIYN dome create a harsh environment for telescope mirrors.

### 5.3 Telescope Guiding and On-Chip Tip/Tilt corrections

Telescope guiding with ODI is facilitated by the instrument itself. ODI uses the focal plane itself to provide telescope guiding capabilities; the guide signal is acquired by using one or more cells with a bright star in video mode. Preferentially an outlying detector outside the central science field is used. The guide star video is then analyzed by the ODI telescope guider application. First the guider waits for the shutter to fully open, as indicated by the detection of guide stars, and then locks the initial position of the guide stars by averaging the star's position for typically 5 seconds. After that, any deviation of the guide stars' mean position with respect to their reference position is then forwarded to the telescope control system as a guide signal. An unavoidable drawback of this approach is that telescope guiding operates only when the shutter is open, i.e., between exposures the telescope is tracking blindly. ODI also fully supports non-sidereal guiding for observations of moving objects; the reference position of the guide star ensemble will be shifted according to the non-sidereal track rate and hence cause the telescope to drift with the prescribed speed.

At this time, guide stars are manually selected from a 1 second "preimage" taken prior to every guided science exposure. However, software predict and automatically select guide stars from a guide star catalog has been successfully tested and is operational. Its practical use is limited by the telescope's pointing and blind tracking accuracy; mitigating the pointing inaccuracy via a star tracker camera is discussed in an accompanying paper at this conference.

**Coherent correction mode:** Although a detector being used for video acquisition (guiding) cannot also be used for the science integration due to the bright output amplifier glow, ODI can still benefit from the orthogonal transfer capability of the OTA detectors: Instead of applying a localized atmospheric image motion correction on the devices, the image motion sensed by a few sacrificial guide detectors can be averaged and then globally applied to the focal plane. This *coherent* correction mode will act as a high-speed telescope guider and can compensate for telescope guide errors at a higher bandwidth than the telescope servo system.

Coherent image motion correction has been functionally tested at ODI and operated at a maximum guide rate of 25 Hz. This guide rate is sufficient to, e.g., correct for the first resonant frequency of the telescope structure at 8 Hz. To achieve this guide rate, exposure times for the guide stars need to be short, and hence will be impacted by the low light level CTE to the fullest extent. In practice, guide stars need to be about 2 magnitudes brighter (12-13 mag) than initially expected. Due to the lack of a sufficient number of guide stars at that magnitude range, the coherent guide mode has not yet been used in routine operations of pODI. As the low light level CTE has been corrected in the Lot 7 OTA design, we expect that coherent guide mode can be fully explored with the updated ODI instrument.

## 6. DATA PROCESSING

Raw data from an exposure are initially stored as a directory of multi-extension FITS files on a local disk at the observatory. Each raw exposure is comprised of 13 FITS files (one for each OTA detector in pODI), each containing 64 extensions (one for each cell in a given OTA). When an exposure is written to disk, a series of automated functions are initiated. First, the raw exposure is processed locally using the QuickReduce<sup>16,17</sup> pipeline, a series of Python-based data reduction routines, performed using archived calibration frames. The bias and dark-subtracted, flat-fielded exposure is written to the local disk, allowing the observer the ability to review a preliminary version of the calibrated data. The QuickReduce pipeline can also perform astrometric and photometric calibration on the fly to support observers identifying faint sources and monitor the sky transparency throughout a night.

Immediately after an exposure is finished, the raw data are transferred to and ingested into the ODI Portal, Pipeline, and Archive (PPA) system, hosted by the Pervasive Technology Institute at Indiana University. The data transfer is managed using the DTS protocol.<sup>18</sup> A full description of the functionality of the ODI-PPA system can be found in a companion paper,<sup>19</sup> but a brief summary follows here. Through the ODI-PPA website, data can be processed via two pipelines, the IRAF<sup>20</sup>-based Automatic Calibration Pipeline (AuCaP), a series of Image Reduction and Analysis Facility based routines developed at the National Optical Astronomy Observatory, and the aforementioned QuickReduce pipeline. The pipelines are given raw science exposures, as well as calibration frames (biases, darks, flat-fields). The pipelines also remove various artifacts from the raw images including fringes, bad pixels, and pupil ghosts (the latter currently under development). The AuCaP pipeline can also automatically produce stacks when more than one of the single exposures are co-located on the sky. The data products (both the single exposures and stacks) are reviewed by the pipeline operator, who can release the final products to the user. All raw and calibrated data products are archived and distributed to the PI and other authorized users. All pODI data become public after 18 months.

In addition to being a platform for the processing and distribution of raw data and calibrated data, the ODI-PPA system also contains functionality for users to perform limited analysis of their data, as well as download raw or calibrated data. A number of user-initiated functions are under development, including the capability to create custom stacks, and to run the QuickReduce pipeline on raw data using customizable parameters.

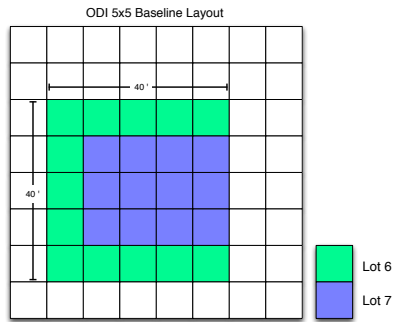


Figure 8. Proposed layout for the ODI focal plane with the addition of 12 more devices.

## 7. UPGRADE PATH AND FUTURE OF ODI

Based on the demonstrated capabilities of pODI, the WIYN science community has given a high priority to upgrading ODI's focal plane with respect to both the detector performance and the field of view. The two remaining key issues of ODI's OTA detectors are amplifier glow and the low light level CTE. The amplifier glow has been sufficiently mitigated by controlling the amplifier's output drain voltage during integration, however, at the expense of giving up the ability to correct for localized atmospheric image motion where a guide star on each detector would be required. Given funding and time requirements to address the amplifier glow, the WIYN science community has abandoned localized image tip/tilt correction. Applying a global tip/tilt correction to correct guide errors and wind shake motion remains a priority.

While amplifier glow has little impact on current pODI science, the low light level CTE issue impacts observing significantly enough that a detector design change was applied and tested. As described earlier, the latest design revision, Lot 7, has fully mitigated the low light level CTE.

The option of abandoning OTA detectors in ODI in favor of conventional, monolithic detectors has been considered as an alternative upgrade path. While proven to be scientifically useful for WIYN, ODI's OTA detectors have significant disadvantages over classical CCD detectors (such as the fragmented imaging area), especially when considering that the main intended benefit, correcting atmosphere-induced image motion, has not been realized in practice. Conventional CCDs benefit from a larger accumulated research and development effort and hence the technology is much more mature. However, the incremental cost (i.e., not accounting previous investment into the initial development of OTA detectors) to add additional OTA detectors to ODI's focal plane is significantly smaller than acquiring commercially available CCDs. The upgrade path using conventional CCDs was therefore found to be not of interest for the WIYN Observatory at this time.

The University of Arizona Imaging Technology Lab is currently processing the remaining Lot 7 detector dies with an expected delivery at the end of 2014. Given previous processing yields, we expect to receive of order of 12 new Lot 7 detectors to augment the current focal plane. The baseline configuration will be to populate the central imaging area with Lot 7 detectors to provide a contiguous area where the CTE issue is mitigated. pODI's thirteen Lot 6 detectors currently will be relocated around that central area to provide a larger overall field of view. All the detectors combined will provide a  $5 \times 5$  detectors array with a total field of view of  $40' \times 40'$ .

As of this writing, decommissioning of pODI for the upgrade is planned for the second half of November 2014, and installation of the upgraded focal plane (called 5x5ODI) is scheduled for May 2015. Upgrading ODI beyond 5x5ODI remains subject to funding and scientific interest in WIYN community.

## 8. SUMMARY

The deployment of pODI at the WIYN 3.5m telescope has validated key components of the ODI instrument concept and its associated data handling process. Most importantly, the instrument fulfills the promise of atmosphere-limited image quality over a one degree field of view and provides a new, scientifically productive capability at the WIYN observatory. The detector performance, when tailored towards static imaging, is adequate to support most science applications, but improvements in the low light level CTE of the new Lot 7 detectors will be a significant improvement over the current state.

Global on-chip tip/tilt image motion compensations has been successfully demonstrated with pODI and will be further developed in the context of 5x5ODI. Nevertheless, both ODI<sup>1</sup> and the PanSTARRS<sup>10</sup> focal planes were initially designed to improve the median image quality by beating atmospheric image distortion with a "rubber focal plane";<sup>12</sup> this promise remains to be fulfilled in production systems. While cost-effective and scientifically productive overall, OTA detectors remain an interesting curiosity for specialized applications and may not be the best choice for wide-area survey instruments.

## ACKNOWLEDGMENTS

## REFERENCES

- [1] Jacoby, G. H., Tonry, J. L., Burke, B. E., Claver, C. F., Starr, B. M., Saha, A., Luppino, G. A., and Harmer, C. F. W., "WIYN One Degree Imager (ODI)," in [*Survey and Other Telescope Technologies and Discoveries*], Tyson, J. A. and Wolff, S., eds., *Society of Photo-Optical Instrumentation Engineers (SPIE) Conference Series* **4836**, 217–227 (Dec. 2002).
- [2] Muller, G. P., Harbeck, D., Jacoby, G. H., Harmer, C., Yeatts, A., Blanco, D., Cavin, J., and Sawyer, D., "Mechanical design of the WIYN One Degree Imager (ODI)," in [*Society of Photo-Optical Instrumentation Engineers (SPIE) Conference Series*], *Society of Photo-Optical Instrumentation Engineers (SPIE) Conference Series* **7014** (Aug. 2008).
- [3] Jacoby, G. H., Harmer, C., Harbeck, D., Muller, G., Blanco, D., Keyes, J., and Cavin, J., "The WIYN One Degree Imager optical design," in [*Society of Photo-Optical Instrumentation Engineers (SPIE) Conference Series*], *Society of Photo-Optical Instrumentation Engineers (SPIE) Conference Series* **7014** (Aug. 2008).
- [4] Harbeck, D. R., Jacoby, G. H., Muller, G., Sawyer, D., Harmer, C., Yeatts, A., Cavin, J., and Corson, C., "The WIYN One Degree Imager: an update," in [*Society of Photo-Optical Instrumentation Engineers (SPIE) Conference Series*], *Society of Photo-Optical Instrumentation Engineers (SPIE) Conference Series* **7014** (Aug. 2008).
- [5] Yeatts, A. K., Harbeck, D., Cavin, J., and McDougall, E., "The WIYN ODI instrument software architecture," in [*Society of Photo-Optical Instrumentation Engineers (SPIE) Conference Series*], *Society of Photo-Optical Instrumentation Engineers (SPIE) Conference Series* **7019** (Aug. 2008).
- [6] Harbeck, D. R., Martin, P., Cavin, J., Jacoby, G. H., Muller, G., Yeatts, A., McCloskey, R., Ivens, J. W., Blanco, D., Corson, C., Gott, S., and Harmer, C., "The WIYN one degree imager: project update 2010," in [*Society of Photo-Optical Instrumentation Engineers (SPIE) Conference Series*], *Society of Photo-Optical Instrumentation Engineers (SPIE) Conference Series* **7735** (July 2010).
- [7] Ivens, J., Yeatts, A., Harbeck, D., and Martin, P., "User interface software development for the WIYN One Degree Imager (ODI)," in [*Society of Photo-Optical Instrumentation Engineers (SPIE) Conference Series*], *Society of Photo-Optical Instrumentation Engineers (SPIE) Conference Series* **7740** (July 2010).
- [8] Yeatts, A. K., Ivens, J., and Harbeck, D., "The WIYN ODI instrument software configuration and scripting," in [*Society of Photo-Optical Instrumentation Engineers (SPIE) Conference Series*], *Society of Photo-Optical Instrumentation Engineers (SPIE) Conference Series* **7740** (July 2010).
- [9] Lesser, M., Ouellette, D., Boroson, T., Harbeck, D., Martin, P., Jacoby, G., Cavin, J., Sawyer, D., Boggs, K., and Bredthauer, R., "Characterization of orthogonal transfer array CCDs for the WIYN one degree imager," in [*Society of Photo-Optical Instrumentation Engineers (SPIE) Conference Series*], *Society of Photo-Optical Instrumentation Engineers (SPIE) Conference Series* **8298** (Feb. 2012).
- [10] Onaka, P., Tonry, J. L., Isani, S., Lee, A., Uyeshiro, R., Rae, C., Robertson, L., and Ching, G., "The Pan-STARRS Gigapixel Camera #1 and STARGRASP controller results and performance," in [*Society of Photo-Optical Instrumentation Engineers (SPIE) Conference Series*], *Society of Photo-Optical Instrumentation Engineers (SPIE) Conference Series* **7014** (Aug. 2008).
- [11] Burke, B. E., Tonry, J., Cooper, M., Luppino, G., Jacoby, G., Bredthauer, R., Boggs, K., Lesser, M., Onaka, P., Young, D., Doherty, P., and Craig, D., "The orthogonal-transfer array: a new CCD architecture for astronomy," in [*Optical and Infrared Detectors for Astronomy*], Garnett, J. D. and Beletic, J. W., eds., *Society of Photo-Optical Instrumentation Engineers (SPIE) Conference Series* **5499**, 185–192 (Sept. 2004).

- [12] Tonry, J. L., Luppino, G. A., Kaiser, N., Burke, B. E., and Jacoby, G. H., “Rubber Focal Plane for Sky Surveys,” in [*Survey and Other Telescope Technologies and Discoveries*], Tyson, J. A. and Wolff, S., eds., *Society of Photo-Optical Instrumentation Engineers (SPIE) Conference Series* **4836**, 206–216 (Dec. 2002).
- [13] Dell’Antonio, I. P. and McCleary, J. E., “Mapping Dark Matter and the PSF: Weak Lensing Studies of Galaxy Clusters with pODI,” in [*American Astronomical Society Meeting Abstracts*], *American Astronomical Society Meeting Abstracts* **222**, 105.07 (June 2013).
- [14] McCleary, J. E., Gilbert, E., and Dell’Antonio, I. P., “Mass and Mass Substructures in Abell 992,” (2014 in prep.).
- [15] Aihara, H. e. a., “The Eighth Data Release of the Sloan Digital Sky Survey: First Data from SDSS-III,” *ApJS* **193**, 29 (Apr. 2011).
- [16] Kotulla, R., “The QuickReduce data reduction pipeline for the WIYN One Degree Imager,” *ArXiv e-prints* (Oct. 2013).
- [17] Kotulla, R., “QuickReduce: Data reduction pipeline for the WIYN One Degree Imager,” (Feb. 2014). Astrophysics Source Code Library.
- [18] Fitzpatrick, M. J., “DTS: the NOAO Data Transport System,” in [*Society of Photo-Optical Instrumentation Engineers (SPIE) Conference Series*], *Society of Photo-Optical Instrumentation Engineers (SPIE) Conference Series* **7737** (July 2010).
- [19] Gopu, A., Hayashi, S., Young, M. D., Harbeck, D. R., Boroson, T., Liu, W. M., Shaw, R. A., Henschel, R., Rajagopal, J. K., Knezek, P. M., Martin, P., and Archbold, K., “ODI-portal, pipeline, and archive (ODI-PPA): A web based astronomical compute archive, visualization, and analysis service,” in [*Software and Cyberinfrastructure for Astronomy III*], *Society of Photo-Optical Instrumentation Engineers (SPIE) Conference Series* (2014 in press).
- [20] Tody, D., “The IRAF Data Reduction and Analysis System,” in [*Instrumentation in astronomy VI*], Crawford, D. L., ed., *Society of Photo-Optical Instrumentation Engineers (SPIE) Conference Series* **627**, 733 (Jan. 1986).